Sixth International Symposium on Turbulence and Shear Flow Phenomena
Seoul, Korea, 22-24 June 2009

LARGE-SCALE DYNAMICS IN THE FLOW AROUND A FINITE CYLINDER WITH GROUND PLATE

Octavian Frederich, Jon Scouten, Dirk M. Luchtenburg, Frank Thiele
Institute of Fluid Mechanics and Engineering Acoustics,
Berlin Institute of Technology
Müller-Breslau-Str. 8, Berlin, 10623, Germany
octavian.frederich@tu-berlin.de

ABSTRACT

To date physically meaningful representations of the non-stationarity in complex 3D flows with converged turbulent statistics are scarce and shed little light on the nonlinear processes in turbulent motion. This study attempts to address part of this deficit by concentrating on the kinematics of larger scales of motion. Two methods are utilised to describe the kinematics of large-scale unsteady motion in the flow around a wall-mounted finite circular cylinder at Reynolds number of $\mathrm{Re}_D = 200\,000$. The first, Proper Orthogonal Decomposition (POD), is a global method resulting in spatial modes defined over the whole domain and their corresponding temporal coefficients. The second, Coherent Structure Tracking (CST), belongs to a class of local methods which extracts connected domains in the flow data.

Based on time coefficients of the first dominant mode pair provided by POD phase-averaging has been performed. Furthermore, modes specific for distinct harmonics are extracted by temporal harmonic filtering. A scalar-field version of CST is proposed yielding an intuitively more accessible description of the flow. The extent to which POD and CST are complimentary is discussed, as well as which partially overlap.

INTRODUCTION

Kolmogorov's similarity hypotheses propose a universal form for the statistics of motion at the smaller scales. No such idea has been suggested for the larger scales. As expounded by Pope (2000), "the energy and anisotropy are contained predominantly in the larger scales of motion", which are geometry-dependent. Physical understanding these coherent structures, which can comprise up to 20% of the energy in the flow, is imperative for dynamic models of the flow field. The harmonics related to the large-scale velocity fluctuations are investigated using POD. Tracking of λ_2 structures yields a vortex structure database, which can later be used to classify types of vorticity formation and their corresponding energy content.

The flow field under consideration is the unsteady turbulent flow around a wall-mounted finite cylinder (see next section). Such configurations have increasingly attracted attention in fluid-mechanical research during the last decades due to relevance as a prototype for many applications, e.g. buildings or fittings on vehicles. There are only few unsteady or time-resolved measurements published for the relatively high Reynolds number $\mathrm{Re}_D = 200\,000$, which can be used for comparison. Especially the dynamic vortex shedding regime with several interacting turbulent phenomena is not adequately described.

Prior to the investigation of the large-scale fluctuations, the configuration and the time-averaged flow are shortly described, followed by a summary of the methods for extracting kinematic information.

FLOW FIELD INVESTIGATED

Central point of the investigations is the flow field around a finite circular cylinder which is mounted close to the leading edge of a ground plate (figure 1). The cylinder with diameter D and length L has an aspect ratio of $L/D = 2$ and the Reynolds number based on diameter, free stream velocity U_∞ and kinematic viscosity ν is $\mathrm{Re}_D = U_\infty D/\nu = 200\,000$. The transition of the plate's boundary layer is fixed by a trip wire near the rounded leading edge of the plate.

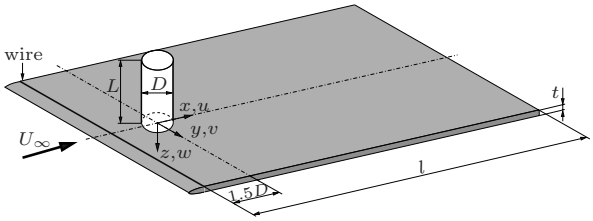

Figure 1: Configuration investigated.

The unsteady flow field has been predicted employing Large-Eddy Simulation (LES) to accurately capture the physics with high resolution in space and time (Frederich et al., 2007a). The LES has been performed with the standard Smagorinsky subgrid scale model where $C_s = 0.1$ using the flow solver ELAN developed at TU Berlin. This code uses a conservative finite-volume discretisation based on general curvilinear coordinates of the Navier-Stokes equations, and is of second order accuracy in time and space (Xue, 1998). The spatial discretisation is block-structured and consists of 12.3 million cells with local block refinement close to the cylinder and in the wake. The time-step for the simulation was $\Delta t = 0.005 D/U_\infty$, whereas the data ensemble contains every 5th time-step within nearly 70 convective units D/U_∞ (2750 snapshots of the full spatially resolved field).

Typical features of the flow field are boundary layer separation, shear layer instability and the subsequent formation of complex vortices, which are strongly affected by downwash effects due to the flow over the free end. The transition on the cylinder shell for the present Reynolds number can be assumed to be fixed by separation (Zdravkovich, 1997). The topology of the time-averaged flow (figure 2) provides starting points for the investigations of the dynamics.

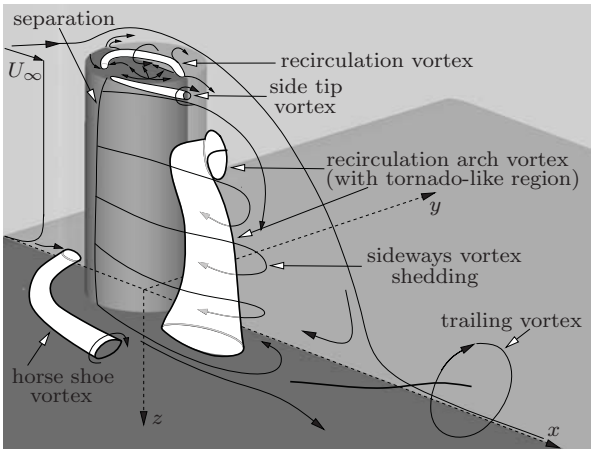

Figure 2: Time-averaged flow topology for the configuration investigated by Frederich et al. (2007a).

METHODS FOR LARGE-SCALE KINEMATICS

In this section, the two methods employed, POD and CST, are described. Both are intended to extract the large-scale coherent structures of the flow field, but with significant difference of the underlying conceptions of coherence.

Proper Orthogonal Decomposition

POD decomposes the flow field in an orthonormal system of spatial modes $\phi_m(x)$ and corresponding temporal coefficients $a_m(t)$. The application of the POD to the M snapshots yields an optimal, in an energetic sense, basis set (Holmes et al., 1996). The decomposition is given by

$$\phi(x_i,t) = \phi_0(x_i) + \sum_{m=1}^{M} a_m(t)\phi_m(x_i) \qquad (1)$$

where ϕ_0 is the ensemble average of the snapshots. Note that the time t and the coordinate x_i are discrete for the current data ensemble.

The method of snapshots by Sirovich (1987) is used to compute the POD in the temporal domain. POD requires the solution of an eigenproblem associated with the correlation matrix C_{mn}. The matrix entries correlate the fluctuation parts $\phi'(x_i,t) = \phi(x_i,t) - \phi_0(x_i)$ of two snapshots at time t_m and t_n in the spatial domain Ω.

$$C_{mn} = \frac{1}{M} \int_\Omega \left[\phi'(x_i,t_m)\phi'(x_i,t_n)\right] \mathrm{d}x_i \qquad (2)$$

The spatial inner product is approximated with a suitable quadrature rule. Here, a simple midpoint rule is used.

The eigenvectors of the matrix C_{mn} are the temporal coefficients $a_m(t_n) = [a_m(t_1) \dots a_m(t_M)]$, which are scaled appropriately.

$$\overline{a_i a_j} = \frac{1}{M} \sum_{m=1}^{M} a_i(t_m)a_j(t_m) = \lambda^i \, \delta_{ij} \qquad (3)$$

The POD modes are computed using the time coefficients as snapshots weights.

$$\phi_m(x_i) = \frac{1}{M\lambda^m} \sum_{n=1}^{M} a_m(t_n)\, \phi'(x_i,t_n) \qquad (4)$$

The POD yields modes describing large-scale coherent motion arising from turbulent kinetic energy and coefficients that can be used to study their temporal evolution.

Coherent Structure Tracking

Examples for searching connected domains in the flow data are the level set method (Osher and Fedkiw, 2001) and Lagrangian coherent structures (Haller, 2002). The CST algorithm presented has been developed by Scouten (2009) and comprises the five major steps specified in figure 3.

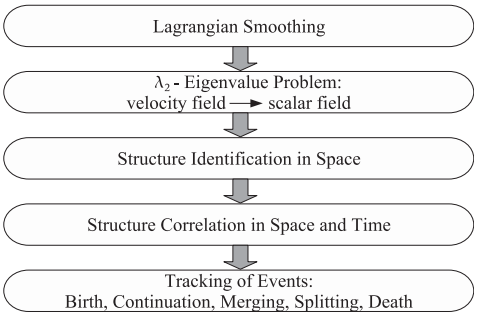

Figure 3: Workflow of the Coherent Structure Tracking algorithm.

Smoothing and filtering the flow field is necessary to track individual vortex structures by the correlation of two consecutive snapshots. The particle tracking required for filtering (and also used to investigate flow dynamics) is performed using an embedded Runge-Kutta-Fehlberg integration scheme with 4th-order accuracy and velocities taken from cubic interpolation in space and time. The averaging along the particle pathlines is performed in two steps: first particles are tracked over 7 timesteps (3 forward and 3 backward), and second the averaging is performed taking 8 pathlines passing through the vertices of a cube in the middle time-step. The advantage of this approach is that it uses the Lagrangian velocity field itself to perform the smoothing away of small scales dynamically, while preserving coherent motion at the larger scales.

The correlation in space and time is calculated between topologically connected domains, which are uniquely identified in each snapshot by a value of the λ_2-vortex-criterion lower than a chosen threshold, here -30. A minimum volume size for the structures of $3 \cdot 10^{-4} D^3$ has been chosen. Additionally, the distance between neighboured points in a vortex domain have to be within a critical distance of $0.03D$, which enables separated structures. The correlated minimum volume between two structures has to be larger than 0.2 to consider these structures as continuation in time. These assumptions are possible due to the high temporal resolution of the LES data. Successful correlations, also occuring between three and more domains simultaneously, are finally sorted by events: birth, continuation, merging, splitting and death; and collected into coherent structures.

POD-Based Evaluations

The unsteady flow field contains a dominant frequency, e.g. in the spectrum of the side force coefficient, which varies

slightly around the Strouhal number of $\mathrm{St} = fD/U_\infty = 0.16$ (slope of curve in figure 4 right). This harmonic is essentially captured by the first POD mode pair. The associated time coefficients a_1 and a_2 describe this harmonic via sine- and cosine-like curves, which are used to define a phase angle $\Phi(t)$ (figure 4). The phase portrait has been divided into intervals to perform phase-averaging of all captured snapshots.

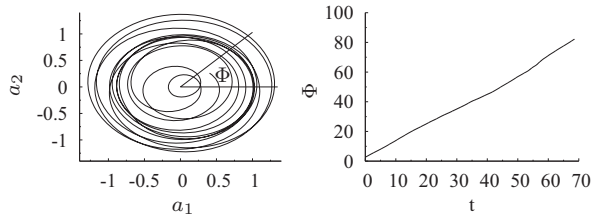

Figure 4: Phase diagram of POD time coefficients a_1 and a_2 (left); instantaneous phase angle $\Phi(t)$ (right).

In general, POD is not able to separate frequencies for three-dimensional, complex flows. Nevertheless a clear decomposition of frequencies is found for the dominant mode pair. In order to ameliorate the frequency separation new spatial POD modes were computed based on the time coefficients convoluted with a windowed frequency taken from the system, either fixed or dynamic. The principle of this filtering approach has been proposed by Tadmor et al. (2008) as Temporal-Harmonic specific POD mode extraction (TH-POD). The time coefficients have been filtered with the varying harmonic described by the dominant POD mode pair (figure 4) and also with different fixed frequencies found in spectral analysis of the time coefficients. Subsequently new modes are recomputed based on an existing low-dimensional description of the snapshot ensemble, which consists of the first 200 POD modes. The fraction of kinetic energy represented by these 200 modes is 95.8%.

SELECTED RESULTS

The presented results focus on the coherent motion in the wake of the cylinder. Time-averaged results including surface quantities have been published recently in Frederich et al. (2007a, 2008a). Database variations w.r.t. domain size and temporal resolution in the framework of POD have been carried out by Frederich et al. (2007b) in order to investigate the effect on the resolved frequency content. The results revealed that the information entropy in the time coefficients decreases with increasing database size. Thus, all the presented POD results are based on the computationally expensive grid of the LES (12.3 million cells) and all available snapshots (2750). An excellent agreement was obtained between LES and the time-resolved measurements by Jensch et al. (2008), including a weighted POD of the velocity field in a PIV measurement plane (Frederich et al., 2008b).

Large Scales Related to Energy

The complexity of the turbulent flow field around the finite cylinder at $\mathrm{Re}_D = 200\,000$ is directly reflected by the POD. The first 123 modes capture 90% of the fluctuating energy, and 99% resolution requires 353 modes (of a total of 2750 modes). Nevertheless, there is at least one clear dominant mode pair [1,2] with a Strouhal number of $\mathrm{St} = 0.16$. This mode pair represents vortex shedding in the wake of the cylinder, whereby an obvious correlation between the sideways vortex shedding from the cylinder shell and the strongly distorted vortices in the far wake exists (cf. figure 6). The experiments of Jensch et al. (2008) reveal the same dominant Strouhal number associated with a vortex street.

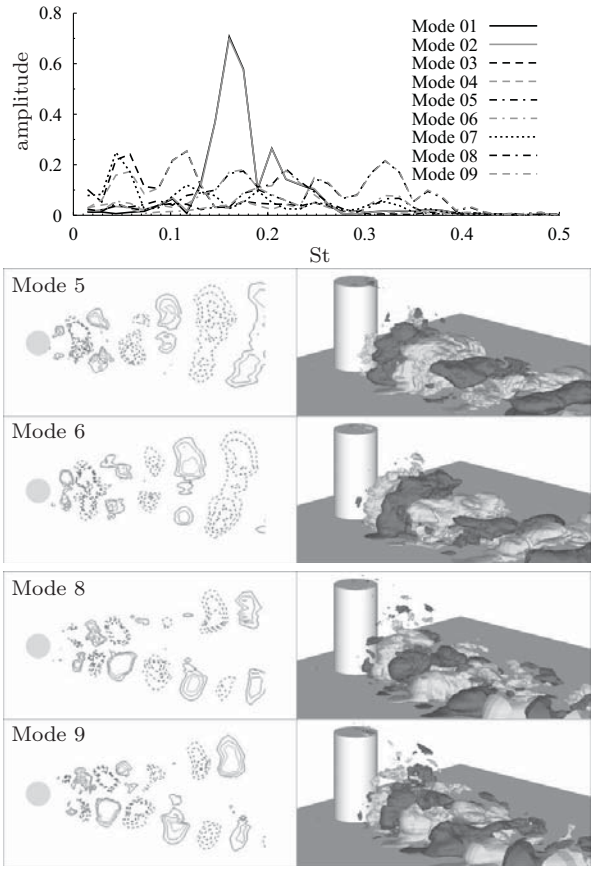

Figure 5: Results of POD based on the original LES-grid: Spectra of time coefficients (top); contour lines in plane $z/D = -0.5$ and isosurfaces of lateral velocity $v = \pm 0.12$ of mode pairs [5,6] (middle) and [8,9] (bottom).

In mode pair [3,4] a subharmonic has been identified which describes symmetrically pulsating changes (w.r.t. the x-z-plane) of the mean near-wake size in all spatial directions. The time coefficients reveal at least two important Strouhal numbers for this harmonic, 0.115 and one half of it. Park and Lee (2000) attributed the former frequency to the downwash from the swirling vortices, which might be the cause of the changing wakesize.

The second harmonic mostly occurs in two mode pairs, [5,6] and [8,9]. Whereas the modes [5,6] are mainly symmetric with respect to the lateral velocity, modes [8,9] are antisymmetric to it (cf. figure 5). The time coefficients of both mode pairs involve several frequencies, this suggests that nonlinear interaction is formed in these modes. Especially, the symmetry of mode pair [5,6] together with spectral portions at twice the Strouhal numbers of 0.115 and 0.16 (0.23 and 0.32) support this hypothesis. This frequency mixing is the motivation for the frequency filtering procedure below (see section “Filtering”).

Mode 7 and higher order modes exhibit a range of different frequencies without evidence of clear mode pairing, and interpretation of their physical relevance is difficult.

Dominant Vortex Motion via Phase-Averaging

The phase angles defined by the time coefficients a_1 and a_2 (figure 4 left) have been subdivided into 16 intervals, each of $\pi/8$ wide, and the snapshots have been assigned correspondingly and averaged. Each interval contains between 164 and 179 snapshots (average is 172), that are used to compute an averaged snapshot for all intervals. These snapshots are mean values related to the mid phase angles $\Phi_{01}..\Phi_{16}$. In figure 6 isosurfaces of the phase-averaged pressure fluctuation are shown for different phase angles, representing the dominant vortex regions. From this visualisation it is evident, that the alternating vortices, which are distorted heavily in the far wake, evolve from the sideways separation. The distortion can be interpreted as vortex overturning due to the intense downwash in the middle wake.

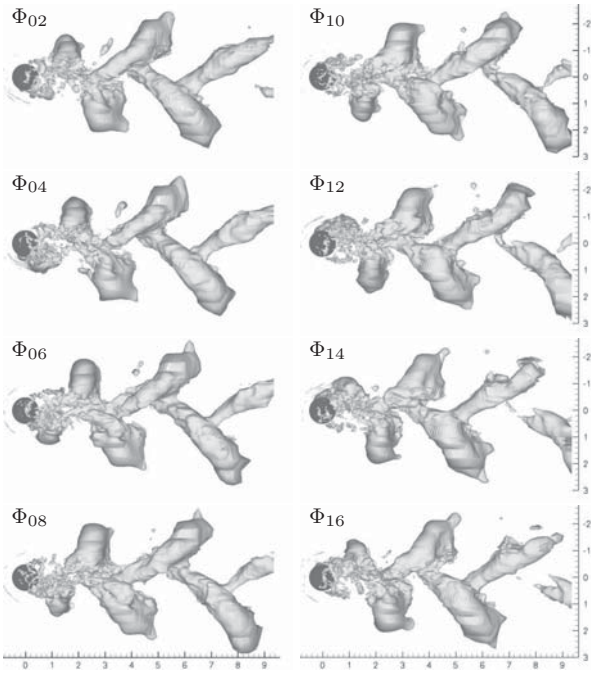

Figure 6: Isosurfaces of phase-averaged pressure fluctuation $\langle p \rangle - \overline{p} = -0.025$ for phase angles $\frac{\pi}{4}, \frac{\pi}{2}, .., \frac{7\pi}{4}$ (topview).

Temporal Harmonic Filtered Modes

The most interesting frequencies follow from the spectra of the dominant POD time coefficients (figure 5 top). Besides the fluctuating frequency defined by the temporal coefficients of the first mode pair [1,2] three (fixed) Strouhal numbers have been chosen for harmonic filtering, namely St = 0.115, 0.167 and 0.20. Since the windowed convolution of the TH-POD acts like a band-pass filter and the tested frequencies are close together, the frequency separation only succeeds partially. Particularly, the predominance of the first mode pair cannot be filtered out, however the high frequencies have been eliminated such that the pairing of the reconstructed modes is highlighted. (cf. figure 5 top and 7). Furthermore, 99% of the kinetic energy represented by the filtered coefficients is contained in the first 50 modes. This means that only the large scales, typically associated with relatively low frequencies, remain after filtering.

Whereas the spatial and temporal parts of the first dominant mode pair hardly changes after filtering and reconstruction, the original mode pair [5,6] is composed with additional fractions of other modes and shifted to position [3,4] for all Strouhal numbers that are used for the temporal filtering cases with one exception. In the case of filtering with

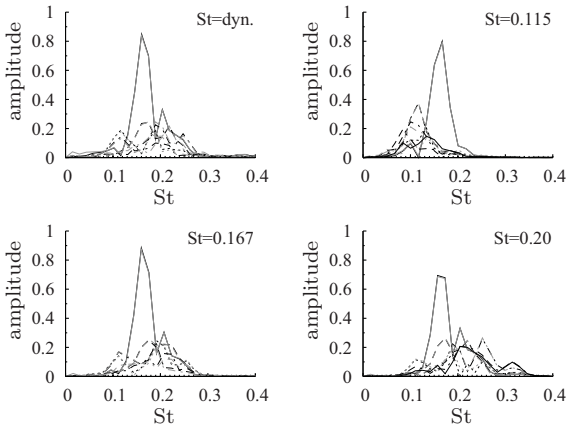

Figure 7: Spectra of filtered time coefficients for the first 10 reconstructed modes and different filter frequencies.

St = 0.115 the original pair [3,4] is reconstructed such that the spectrum of the corresponding time coefficients has just a single (though broad) peak at this Strouhal number, and no re-sorting to the energy fraction contained is necessary. Furthermore, as a result of the filtering at the same Strouhal number the spectral peak of mode pair [1,2] at St = 0.20 has nearly been eliminated.

The filter effectivity of the latter filter at the Strouhal number St = 0.20 for the mode [1,2] can also be quantified for the spatial mode. The vector field difference between the normalised POD and the filtered modes is calculated, in order to extract the scales connected to St = 0.20. Certainly, the new vector field contains nonzero differences in the entire wake, which grow in size with advancing streamwise direction due to the turbulent spreading. It also contains high-frequency content which has been filtered out. However the most important part of this difference velocity field comprises vortex shedding. Since the Strouhal number St = 0.20 is typical for undisturbed vortex streets behind infinite cylinders (Zdravkovich, 1997) and is also found predominantly in the lower part of long finite cylinders (Park and Lee, 2000), it has been presumed that the related structures originate from the undisturbed sideways separation. In fact, the velocity magnitude of the difference field does not only confirm this, but also allows to localise the region of undisturbed shedding with St = 0.20. The isosurface shown in figure 8 reveals the existence of this region up to two thirds of the cylinder height. It is important to notice, that the combination of the mode differences describes a dynamic region with travelling wave character. The further parts of the isosurface attached to the cylinder, especially on the top, are associated to different, primarily higher frequencies.

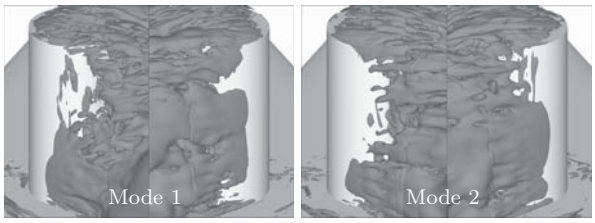

Figure 8: Velocity magnitude as difference between modes 1 (left) and 2 (right) of the basic POD and filtered with St = 0.115; isosurface $\Delta U = 0.025$ shown from positive and negative lateral direction, respectively.

As mentioned for the standard POD, the mode pair [3,4] involves a dominant frequency at St = 0.115, which has been

addressed to features arising from the flow over the top. Considering the importance of these two modes, expressed by their position in the mode order, their connection to this part of the flow becomes apparent, because the free end flow and the caused downwash behind the cylinder are dominant global flow phenomena. After filtering with the distinct frequency the spectra of the related time coefficients are cleaned towards a small frequency band.

The filtered mode pair [3,4] describes complex structures, which are difficult to interpret physically. This is probably due to the global correlation of POD, which makes it hard to interpret compact (local) physical phenomena. An intermediate phase-averaging based on the time coefficients' phase reveals again a pulsating change in wake size. The predominant symmetry of the modes especially affects the streamwise location of the reattachment point on the plate. The wake length and width seem to periodically vary with it. The flow over the top participates in these variations, but currently no proof can presented, that this movement causes the fluctuations. It is worth mentioning here, that the position and size of the tip vortices is relatively steady and therefore mainly included in the mean flow. However, the field described by the modes comprises a variety of streamwise vorticity. Figure 9 shows the velocity components necessary for streamwise rotation.

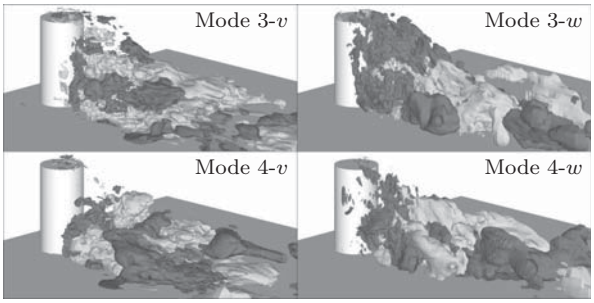

Figure 9: Isosurfaces ± 0.1 of lateral (left) and vertical velocity components (right) for modes 3 (top) and 4 (bottom) after filtering with St = 0.115 (− dark, + light).

Tracking of Coherent Vortex Regions

While POD searches for global correlations and extracts coherent structures, which exist statistically over time, CST identifies and tracks the motion of instantaneous coherent fluid. The CST method given here filters out small scales, thus imposing a critical minimum vorticity concentration. This implies that a structure is lost if the critical concentration not maintained. Conversely, this feature provides to a certain extent the detection of local vorticity formation.

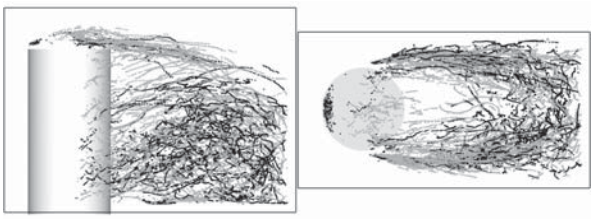

Figure 10: Reduced domain for tracking (box) and trajectories of structures with lifetime of 1.75...2.5 (light) and > 2.5 (dark) w.r.t. D/U_∞ (side and topview).

In the first step CST has been employed for tracking structures in a reduced domain including the sideways shear layers, the cylinder top and the near wake (figure 10). Consistent with observations in instantaneous snapshots, the identified structures are relatively small in size and have a duration of maximally 3 convective time units. The centroids (geometric middle-points) of the structures found with the CST algorithm are used to visualise the pathlines, shown in figure 10. As an example of structures tracked, the pair of tip vortices shown in figure 11 illustrates the separation from the cylinder top and also from the sides.

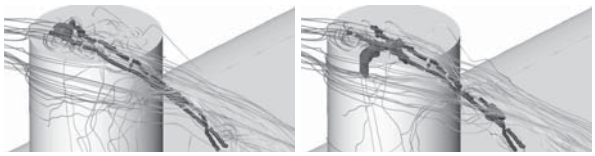

Figure 11: Exemplarily tracked structures near the top of cylinder with their trajectories and instantaneous streamlines: temporal stages shifted by $0.5D/U_\infty$.

As explained, CST can be used to detect vortex formation, thereby assisting the exploration of three-dimensional and unsteady flow data with complex turbulent regime. In this way, an important instantaneous flow feature could be studied, which could not represented by the mean flow. Figure 12 top-left shows a pathline with the tracked structure at mid lifetime and its center located at $(x, y, z)/D = (1.53, 0.26, -0.39)$. The inspection of the corresponding flow field reveals a nearly streamwise oriented vortex formation with flow direction towards the cylinder (cf. figure 12 top-middle and bottom-right). This vortex is found in the gap between the newly evolving and already downstream convected shedding vortices, and in lateral direction opposite to the alternate counterpart depicted by isosurfaces of the instantaneous pressure in figure 12 top-right.

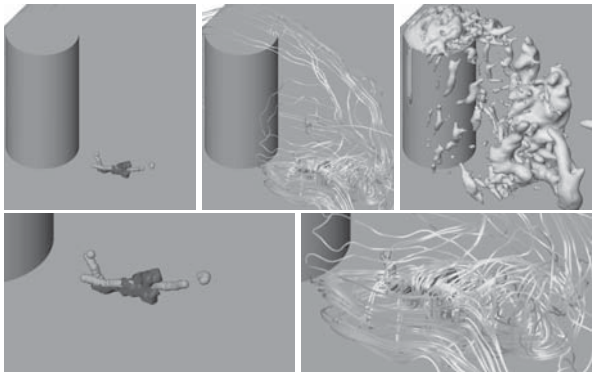

Figure 12: Instantaneous vortex formation: tracked structure with trajectory (left), streamlines (middle), isosurface of pressure (right) and enlarged details (bottom).

The total tracking time of this structure is $2.65D/U_\infty$, which is within the time frame of the half dominant shedding period $3.125D/U_\infty$ (St=0.16). A survey of further pathlines and snapshots manifested the occurrence of such vortex formations on both sides at similar spatial and phase positions w.r.t. the dominant shedding. The developing vortices are directly connected to and fed by the flow over the top (figure 12 top-middle). Whereas the downwash flow is periodically shifted in lateral direction by the alternate vortices with vertical axis, the combination of both induces the vortex formation discovered. Temporal analysis of the periodic evolution revealed a large variation in size, but also slightly in position and local direction. Since the structure is located in a region of relatively low velocity, it can be safely assumed that these variations follow from nonlinear interaction of the sideways shedding and the downwash flow.

SYNTHESIS

The large-scale coherent motion in a complex flow has been captured by two methods, whose underlying conceptions of coherence differ considerably. The mode pairs resulting from POD reveal large-scale convecting structures related to physically meaningful harmonics. As a result of the global correlation by POD it is however difficult to separate interacting phenomena. This is indicated by the mixing of frequency bands within a single time coefficient. This effect has been partially reduced employing the temporal filtering approach (TH-POD). Unfortunately, the narrow band of several important frequencies in the flow field limits the performance of the method.

In order to analyse unsteadiness without relying on statistics the CST method has been proposed and successfully employed. The basic variant of CST is able to track a variety of different λ_2-structures and can be used as an indicator of vorticity formation. Compared to POD, where all correlations of turbulent fluctuations are sorted globally w.r.t. energetic optimality, CST correlates local vortex regions to extract instantaneous coherent motion. POD allows to detect the primary periodic structures, whereas CST additionally resolves secondary phenomena, and the tracking of global vorticity transport is limited. Nevertheless, it is evident that the qualitative congruence of POD and CST depends on the complexity of the flow, e.g. quantified by frequency separation between POD modes.

The unsteady flow field under consideration has been shown to comprises a dominant vortex street, which starts as sideways shedding at the lower part of the cylinder, and is strongly distorted further downstream in the wake through downwash from the top and boundary effects of the plate. Furthermore, instantaneous secondary vortex formation has been observed in the initial region of the vortex street, which has not been reported in literature before. Within a portion of the recirculation region the observed vortices are oriented nearly streamwise, but with fluid moving towards the separation region of the cylinder. The mechanism responsible for the decrease in Strouhal number for finite cylinders compared to the infinite counterpart is currently not fully understood. It is plausible, that the global recirculation and angular momentum manifested close to instability regions is an important component of the delayed separation.

OUTLOOK

The primary goal is to combine the ability of POD with the intuitively accessible motion of vortex structures provided by CST. The centroid paths will be used to classify the vortex structures and to evaluate quantities such as kinetic and rotational energy in order to construct an energy-based model of the flow. Since some of the global fluctuations are currently unamenable to interpretation, as evident from mode pair [3,4], a POD decomposition of the pressure field has been performed. This pressure field exhibits smoother modes, which might be easier to interpret. The snapshot weights out of this will also be used to construct the velocity field modes, taking advantage of the natural smoothness of the pressure field.

Improvements to the basic CST algorithm and also the filtering procedure of TH-POD are under investigation. Possible modifications are focused to allow vorticity tracking throughout the wake for CST. In the framework of POD the focus is on clearer frequency separation of the coherent structures.

ACKNOWLEDGMENTS

The authors acknowledge the funding provided by the German Research Foundation (DFG) within the scope of the research unit “Imaging Measurement Methods for Flow Analysis” and of the Collaborative Research Centre (SFB 557) “Control of complex turbulent shear flows” hosted at the Berlin Institute of Technology. All simulations were performed on the IBM pSeries 690 supercomputer of the North-German Supercomputing Alliance (HLRN).

REFERENCES

Frederich, O., Wassen, E., Thiele, F., Jensch, M., Brede, M., Hüttmann, F. and Leder, A., 2007a, “Numerical simulation of the flow around a finite cylinder with ground plate in comparison to experimental measurements”, *Notes on Numerical Fluid Mechanics and Multidisciplinary Design*, Vol. 96, pp. 348-355, Springer.

Frederich, O., Scouten, J., Luchtenburg, M. and Thiele, F., 2007b, “Database variation and structure identification via POD of the flow around a wall-mounted finite cylinder”, *Proceedings BBVIV5*, Costa do Sauípe, Brasil.

Frederich, O., Wassen, E. and Thiele, F., 2008a, “Prediction of the flow around a short wall-mounted cylinder using LES and DES”, *Journal of Numerical Analysis, Industrial and Applied Mathematics*, Vol. 3, No. 3-4, pp. 231-247.

Frederich, O., Scouten, J., Luchtenburg, M., Thiele, F., Jensch, M., Hüttmann, F., Brede, M. and Leder, A., 2008b, “Joint numerical and experimental investigation of the flow around a finite wall-mounted cylinder at a Reynolds number of 200000”, *Proceedings ETMM7*, Limassol, Cyprus.

Haller, G., 2002, “Lagrangian coherent structures from approximate velocity data”, *Physics of Fluids*, Vol. 14, No. 6, pp. 1851-1861.

Holmes, P., Lumley, J. L. and Berkooz, G., 1996, *Turbulence, Coherent Structures, Dynamical Systems and Symmetry*, Cambridge University Press.

Jensch, M., Brede, M., Leder, A., Frederich, O. and Thiele, F., 2008, “Use of pod to visualize coherent structures from time resolved PIV data”, *Proceedings LxLaser14*, Lisbon, Portugal.

Osher, S. and Fedkiw, R. P., 2001, “Level set methods: An overview and some recent results”, *Journal of Computational Physics*, Vol. 169, No. 2, pp. 463-502.

Park, C.-W. and Lee, S.-J., 2000, “Free end effects on the near wake flow structure behind a finite circular cylinder”, *Journal of Wind Engineering and Industrial Aerodynamics*, Vol. 88, pp. 231-246.

Pope, S. B., 2000, *Turbulent flows*, Cambridge University Press.

Scouten, J., 2009, *Coherent structure tracking with application to the wake flow behind a wall-mounted finite circular cylinder*, Student project, TU Berlin (under preparation).

Sirovich, L., 1987, “Turbulence and the dynamics of coherent structures”, *Quarterly of Applied Mathematics*, Vol. 5, pp. 561-590.

Tadmor, G., Bissex, D., Noack, B.R., Morzyński, M., Colonius, T. and Taira, K., 2008, “Temporal-Harmonic specific POD mode extraction”, AIAA-2008-4190.

Xue, L., 1998, *Entwicklung eines effizienten parallelen Lösungsalgorithmus zur dreidimensionalen Simulation komplexer turbulenter Strömungen*, PhD thesis, TU Berlin.

Zdravkovich, M. M., 1997, *Flow around circular cylinders, Vol. 1: Fundamentals*, Oxford University Press.